

ROLE OF ZINC IN BULK PRECIPITATION FROM THE STEAMING PROCESS OF POTABLE WATER

A. Al-Gailani^{1*}, M. J. Taylor¹ and R. Barker²

¹ Department of Chemical Engineering, School of Engineering, University of Hull, Hull, HU6 7RX, United Kingdom

² School of Mechanical Engineering, University of Leeds, Leeds, LS2 9JT, United Kingdom

* Corresponding Author: A.Z.Al-Gailani@hull.ac.uk

ABSTRACT

Water chemistry plays an important role in fouling kinetics and morphology. This work investigates the influence of zinc cations in potable water, specifically the kinetics of crystallisation and their effect on the fouling layer during the operation of a batch steam generator system and a once-through flow system. The kinetics of precipitation in the batch crystalliser were examined, based on the change in concentration of the foulants while the fouling resistance approach was used in the flow system. Morphological testing was carried out using Scanning Electron Microscopy, Powder X-ray Diffraction, and Energy dispersive X-ray. The findings showed that the rate of precipitation of calcium carbonate decreases with the increase in zinc ions, until reaching the zinc carbonate supersaturation in the water due to water evaporation. In terms of morphology, co-precipitation of zinc carbonate was observed at high zinc concentrations. As a result, a double effect was observed where zinc both retarded and enhanced fouling over time. The fouling rate in the flow system decreased as the concentration of zinc increased. Zinc ions were found to have a significant influence on the morphology of deposit minerals. Moreover, the surface deposition of zinc salts increased with the solution content of zinc.

INTRODUCTION

The presence of simple metal ions or complex ions in water may pose an inhibitory impact on the nucleation and growth process of mineral scale crystals. Scale is the formation of unwanted solid minerals onto the heat transfer surfaces and bulk solutions, for example inside the piping system, in valves, heat exchangers etc. In household appliances, a composite scale of different minerals (CaCO₃, MgCO₃ and CaSO₄) might form due to the presence of a variety of ionic species in potable water. The understanding of surface deposition and bulk precipitation from potable water in domestic appliances is a real challenge for consumers and manufacturers.

At very low concentrations, cationic additives like magnesium, copper, zinc, lead, manganese, nickel, and iron could adsorb onto the active growth

positions on the precipitate particles [1]. Zinc is present in potable water and surface water at a concentration of up to 15 mg/L. The main sources of zinc in potable and surface water are leached or discharged from steel production by-products (slag) or coal-fired power station waste [2].

Water treatment devices use a scale reducer made of elemental zinc which may corrode, leading to the release of zinc cations (Zn²⁺) into the water. For almost the first time, Coetzee and Howell [3] reported the inhibitory impact of zinc on scale formation. They use three types of physical water treatment methods with low concentrations of Zn²⁺. The inhibitory impact of zinc ions on the bulk precipitation of scale particles has been reported in a few other studies such as Zachara, et al. [4] who emphasized rapid adsorption of Zn²⁺ on calcite (hexagonal calcium carbonate) according to the exchange of Zn²⁺ and ZnOH⁺ with surface-bonded Ca²⁺. However, it has been also confirmed that Zn can react with carbonate ions, forming ZnCO₃ crystals, which enhance the heterogeneous nucleation [5, 6].

In some household devices, steaming is a common practice, leading to unavoidable mineral scaling from potable water. The role of zinc in the crystallisation fouling of inorganic minerals during a steaming process or water boiling has received inadequate attention. During a steaming process, the supersaturation of different inversely soluble minerals is affected by both temperature change and the evaporation of water.

In this work, the effects of zinc ions on the crystallization fouling in the bulk solution and the heated surface from potable water were investigated during the steaming process using two unique experimental setups to mimic different household appliances. A batch configuration can be seen in kitchen kettles and small boilers, while the flow system is dominant among household devices such as central heating.

Varying concentrations of Zn²⁺ were used (0 to 15 mg/L) to examine the impact on the fouling kinetics and scale particle morphology during the steaming process in both setups. The bulk crystallisation of the zinc minerals was studied using spectroscopic analysis. The surface deposition was

examined on an aluminium surface using a fouling resistance approach and deposits mass.

MATERIALS AND METHODS

Batch crystalliser system

The first part of the experiments was conducted using a batch crystalliser in which the precipitated scale particles in the bulk fluid and on the solid surface can be evaluated, as shown in Figure 1. For bulk precipitation kinetics, the turbidity of the solution and concentration of ionic zinc were quantitatively measured. The solution content of Zn^{2+} was measured as a function of time, following an accurate sampling procedure. Also, as the heat was constantly supplied, the bulk temperature increased with time. The solution supersaturation, with respect to mineral salts was reduced with time in such a closed system. This unique setup was developed for mimicking a batch evaporation process in both domestic and industrial systems.

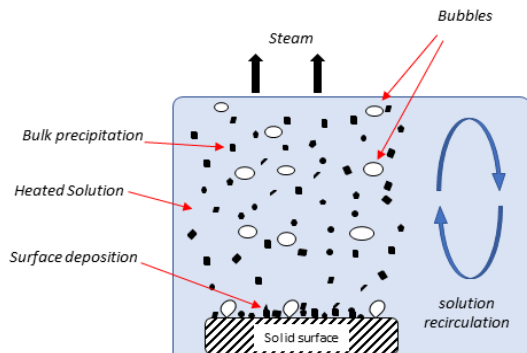


Figure 1. Representation of bulk precipitation in the experimental vessel.

The setup consists of a 1000 mL borosilicate glass beaker, hot plate (Heidolph), Pt1000 thermocouple (ThermoScientific), and metallic samples. The test specimen was constructed of stainless steel 316L (SS31603) for minimizing the potential of corrosion product formation.

Once-through flow system

In this setup, the inorganic fouling of the heat transfer surface associated with partial water evaporation was studied during pool boiling. This setup was an open system where a once-through flow was adopted. Figure 2 illustrates the schematic of surface deposition under the conditions used in the present experiments. The schematic diagram of the experimental apparatus is shown in Figure 3. It consists of a solution tank, peristaltic pump, test flow cell, sample heating system, data acquisition system and waste tank. This once-through flow system was adopted to avoid any reduction in the saturation state which may result from solution recirculation.

Aluminium alloy 1050A ($Al \geq 99.5\%$) was used to fabricate the test specimen which was chosen as it is one of the most common materials used in constructing heat transfer surfaces in household appliances. The influence of the resistive fouling layer on the heat transfer was evaluated using fouling resistance. The design details of the test flow cell, dimensions of test specimens, method of the fouling resistance calculation, data acquisition system and the experimental procedure are reported in our previous work Al-Gailani, et al. [7].

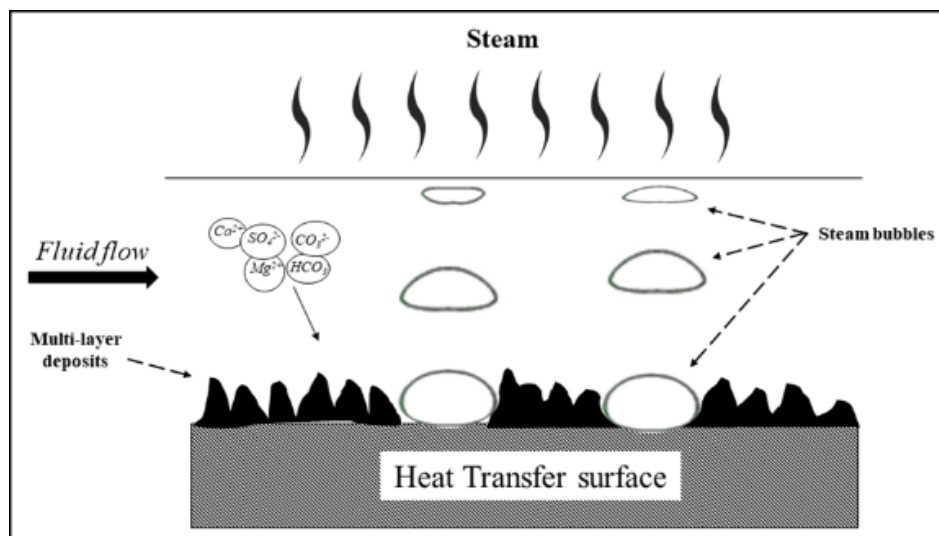


Figure 2. Schematic of surface deposition in the once-through flow system.

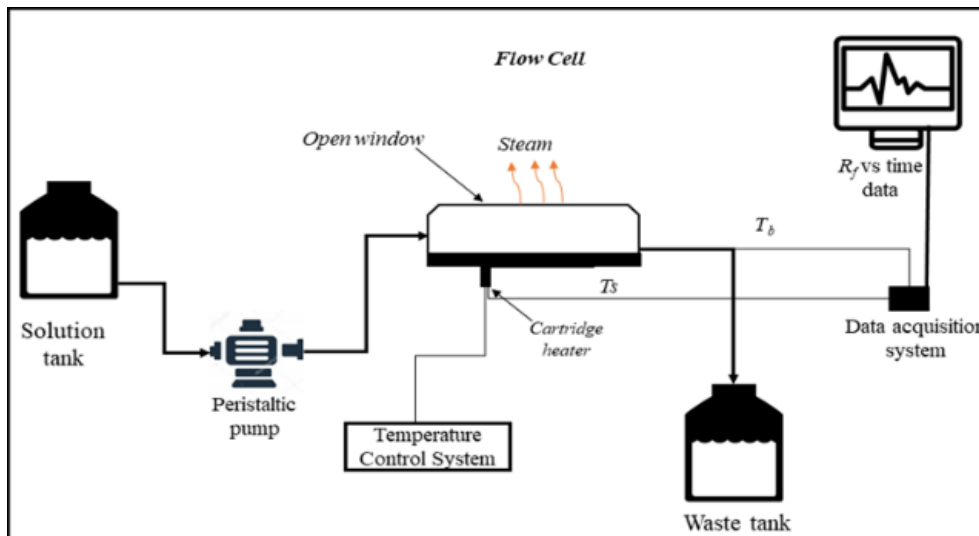


Figure 3. Configuration of the once-through flow system.

The flow cell was designed to obtain a fully developed laminar flow on the tested aluminium surface at an average flow rate of 8 mL/min. The surface temperature was maintained at a constant 100 °C, under atmospheric pressure. The test specimen surface was ground with silicon carbide paper (1200 grit) and then polished with a diamond suspension (0.5 µm) to obtain an arithmetical mean roughness of 22.4 – 31.2 nm.

Test solutions

The base test solution used in both systems is commercially-available bottled water (Evian® Natural Spring Water) with a pH of 7.2. It has been chosen for its hardness due to 307 ppm of CaCO₃, which is almost the same as potable water hardness in some areas of the south of the United Kingdom. The composition of the base solution is listed in Table 1. The main test solutions were prepared by adding Zinc sulphate monohydrate ZnSO₄·H₂O (Sigma Aldrich, Min. 99.9%) to the base solution to produce solutions of 5, 10, and 15 mg/L of zinc.

Table 1. Composition of the base solution.

Ionic species	mg/L
Ca ²⁺	80.0
Mg ²⁺	26.0
Na ⁺	6.5
K ⁺	1.0
Si ⁴⁺	15.0
HCO ₃ ³⁻	360.0
SO ₄ ²⁻	14.0
Cl ⁻	10.0
NO ₃ ³⁻	3.8
Dry residue at 180°C	345.0

For the crystallisation fouling in the batch system, at specific time intervals, 1 mL of the test solution was

taken from the test vessel. The solution volume was mixed with 9 mL of a quenching (KCl/polyvinyl sulfonate) solution to prevent further precipitation [8].

Surface and solution characterisation

At the end of the experiment, the weight of the metallic sample was evaluated, and the surface deposits were characterised. While the 10 mL solution samples were used to assess the bulk concentration of cations (Ca, Zn, Na, Mg, K and Si) by Flame Atomic Absorption Spectrophotometer (AAS) (Agilent Technologies, Model: 240FS AA, USA). Besides the AAS samples, an aliquot of 10 mL was taken at the same time intervals for the turbidity measurements conducted using a DR-890 Colorimeter (CAMLAB). The deposit morphology was examined using a Philips X'Pert X-ray diffractometer (PXRD) (X'Pert MPD, Cu anode x-ray source, Netherlands) and a Carl Zeiss EVO MA15 Scanning Electron Microscope. Samples were coated with iridium (Ir) at a thickness of 10 nm using sputter coating to avoid charge build-up on a sample surface. Energy dispersive X-ray (EDX) elemental analysis was used to determine the composition of scale particles.

RESULTS AND DISCUSSION

Fouling crystallisation in the Batch system

The effect of Zn²⁺ on the bulk crystallisation of inorganic minerals from potable water was studied. Figure 4a displays the profile of Ca²⁺ concentration during heating of the zinc-containing potable water from room temperature to boiling under atmospheric pressure. In the zinc-free solution, the content of Ca²⁺ decreases at a temperature of ~57 °C after 5 min of heating. The time taken for Ca²⁺ (induction time) to reduce is prolonged as the Zn²⁺ content increases. On contrary, the concentration of Ca²⁺ increases to a

maximum point due to water evaporation with temperature increase. This maximum point in the Ca^{2+} concentration profile represents the supersaturation of CaCO_3 with respect to temperature and solution volume. However, it decreases when attaining the required supersaturation for the scale to precipitate. The Zn^{2+} in solution complexes with the carbonate fouling species, increasing the energy barrier of the crystallisation reaction [9-11]. It has been reported that zinc may react with CO_3^{2-} resulting in the formation of stable ZnCO_3 , competing with Ca^{2+} [5].

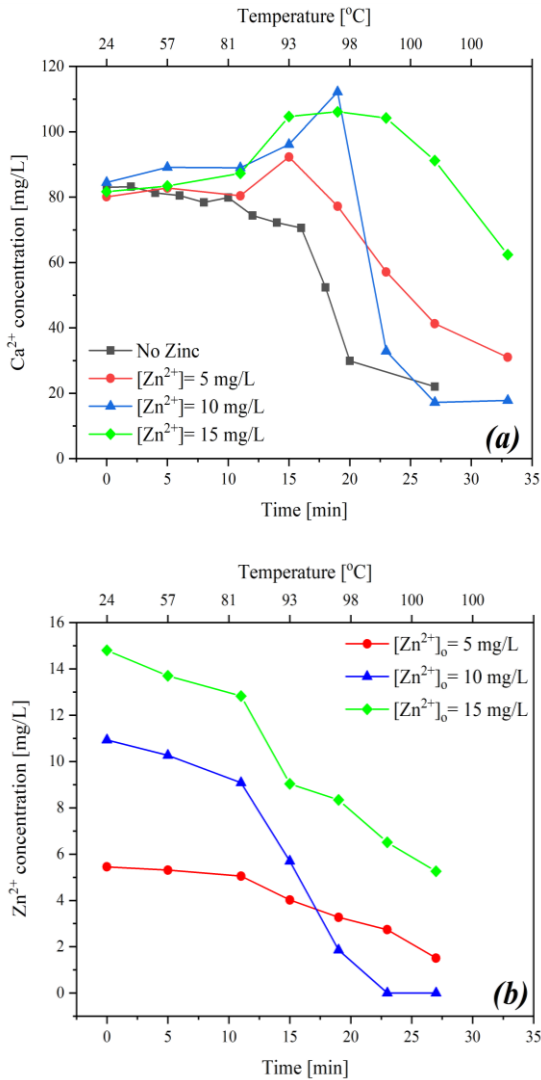


Figure 4. (a) Ca^{2+} concentration profile and (b) Zn^{2+} concentration profile, during water heating for different ZnSO_4 concentrations.

The sharp reduction in the Ca^{2+} concentration for cases with Zn^{2+} indicates that zinc inhibition has ended. The AAS analysis in Figure 4b shows that Zn^{2+} concentration in the solution decreases with temperature and time. It is expected that the Zn^{2+} to increase due to the evaporation of water as the temperature increases. The zinc ions are involved in

reactions with the fouling species for the formation of zinc minerals or inhibiting precipitation of other minerals. Forming a complex with HCO_3^- , CO_3^{2-} and Ca^{2+} might be the case in the first period of heating ($<85 \text{ }^\circ\text{C}$) [9]. However, for steeper depletion in Zn^{2+} ($>85 \text{ }^\circ\text{C}$), the crystallisation of ZnCO_3 occurs [12].

The results of the Ca^{2+} profile at different zinc concentrations were interpreted into the crystallisation induction time, as shown in Figure 5a. The time taken for the first visible crystal to appear in the bulk solution, the induction time, increases exponentially with an increase in zinc content in the water. This confirms that zinc during the initial period of heating forms a complex with the fouling species, preventing the crystallisation reaction [13].

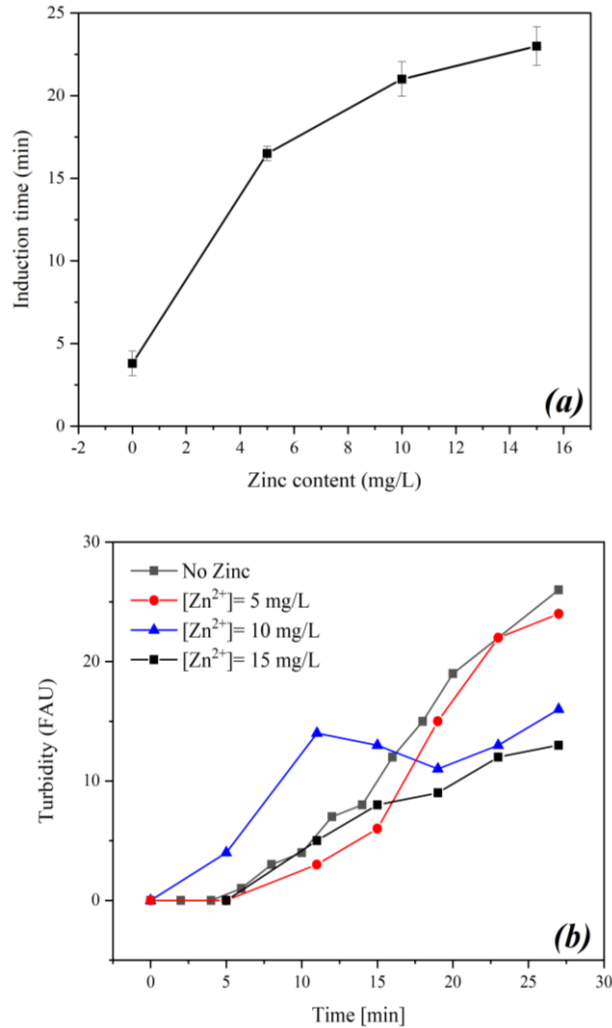


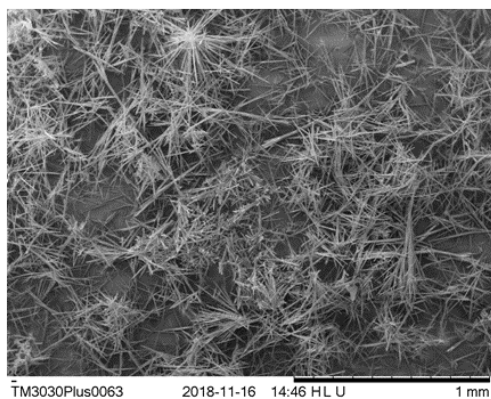
Figure 5. (a) Crystallisation induction time and (b) solution turbidity, for different Zn concentrations.

Figure 5b illustrates the solution turbidity as a function of time for various concentrations of Zn^{2+} . The solution turbidity increases with time for all solutions. However, the turbidity of the high Zn^{2+} solutions (10 and 15 mg/L) is the lowest at the later stages of heating. The turbidity measurement indicates the solution cloudiness caused by the

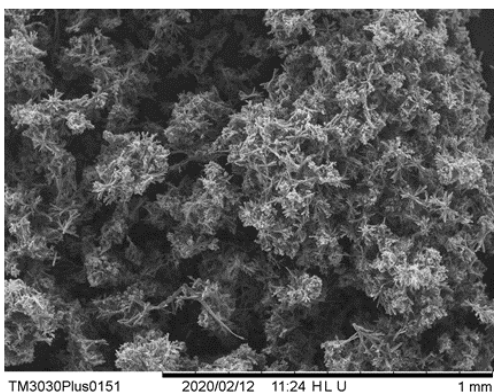
suspended particles of scale. As the density of the ZnCO_3 is 2x that of CaCO_3 , the ZnCO_3 crystals tend to precipitate faster than CaCO_3 or MgCO_3 [14] resulting in less turbidity.

The effect of Zn^{2+} on the scale morphology is presented in SEM and PXRD analysis in Figures 6a, 6b and 7. The SEM observations in Figure 6 show that the deposits with no zinc mostly comprise needle-like aragonite (Orthorhombic CaCO_3). However, at 15 mg/L mineral deposits transform into lumpy crystals which are attributed to the precipitation of ZnCO_3 . The presence of ZnCO_3 as smithsonite was confirmed by PXRD analysis, as shown in Figure 7. A small peak corresponding to ZnO is also observed.

At high concentrations, Zn^{2+} interacts with HCO_3^- or CO_3^{2-} to form zinc inversely soluble salts such as $[\text{Zn}(\text{CO}_3)_2]^{2-}$, $\text{Zn}_5(\text{CO}_3)_2(\text{OH})_6$ and ZnCO_3 [6]. These minerals co-precipitate with other minerals such as CaCO_3 and MgCO_3 . Some minerals like $[\text{Zn}(\text{CO}_3)_2]^{2-}$ are more likely to act as a site for other mineral nucleation and growth. The precipitation of zinc minerals retards the heat transfer as it adds more insulation to the surface.



(a)



(b)

Figure 6. SEM images of (a) the precipitated scale with no Zn in water and (b) with 15 mg/L Zn^{2+} .

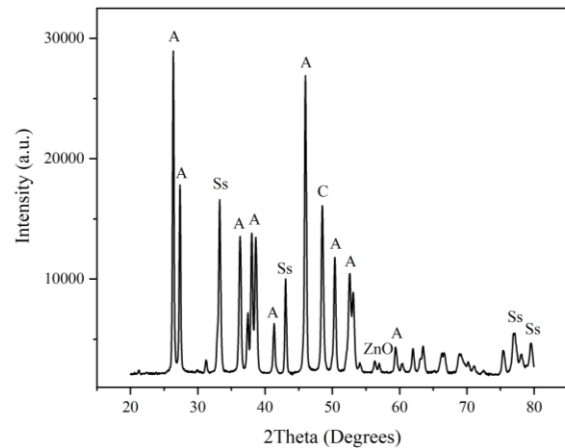


Figure 7. XRD diffractogram of bulk precipitate in presence of 15 mg/L zinc (A: aragonite, C: calcite, and Ss: Smithsonite).

Fouling crystallisation in the once-through flow system

The effect of the free zinc ion has been investigated on the composite crystallisation fouling from potable water. The findings show the thermal fouling resistance drops as the concentration of Zn^{2+} , as shown in Figure 8a. It also illustrates that Zn^{2+} concentration is also capable of affecting the induction time. The asymptotic fouling resistance was reduced by half when the Zn^{2+} concentration increased by 15 mg/L (Figure 8b). The exponential decay of asymptotic fouling resistance refers to the decreasing inhibition efficiency of zinc. It has been reported that the nucleation of CaCO_3 is inhibited by Zn^{2+} with a concentration starting from 0.02 mg/L [15]. For the same range, the mass of deposits decreased by 25.3 mg.

Figure 9a shows an exponential growth relationship between the asymptotic fouling resistance and the scale mass. However, this relationship may indicate variation in the physical properties of the fouling crust such as density, thermal conductivity and porosity. As mentioned earlier, the Zn^{2+} exhibits a pronounced impact on the induction period. The scaling induction time increased from 78 to 426 minutes when the Zn^{2+} concentration raised from 0 to 15 mg/L, as displayed in Figure 9b. The presence of Zn^{2+} in a solution suppresses the nucleation and growth of scale particles through the complexation with the foulants [9-11, 16]. Another inhibition mechanism, the high frequency of adsorption of Zn^{2+} at the nuclei sites may mitigate the nucleation rate [17].

On the other hand, the co-precipitation of zinc carbonate (ZnCO_3) and hydrozincite ($\text{Zn}_5(\text{CO}_3)_2(\text{OH})_6$) crystals may occur at a Zn^{2+} concentration greater than 6 mg/L [5, 6, 17]. The morphology investigations show that the Zn^{2+} has changed the structure of deposits, as displayed in the

SEM images in Figure 10. In the absence of zinc, the deposits from potable water comprise loose needle-like aragonite particles. However, smooth flat islands are found distributed on the flower-like aragonite when 10 mg/L is added to the test solution. At a concentration of 15 mg/L, the formed crystal structure completely changed. This morphology might be resulted from aragonite crystal poisoning with Zn^{2+} and/or co-precipitation of zinc deposits.

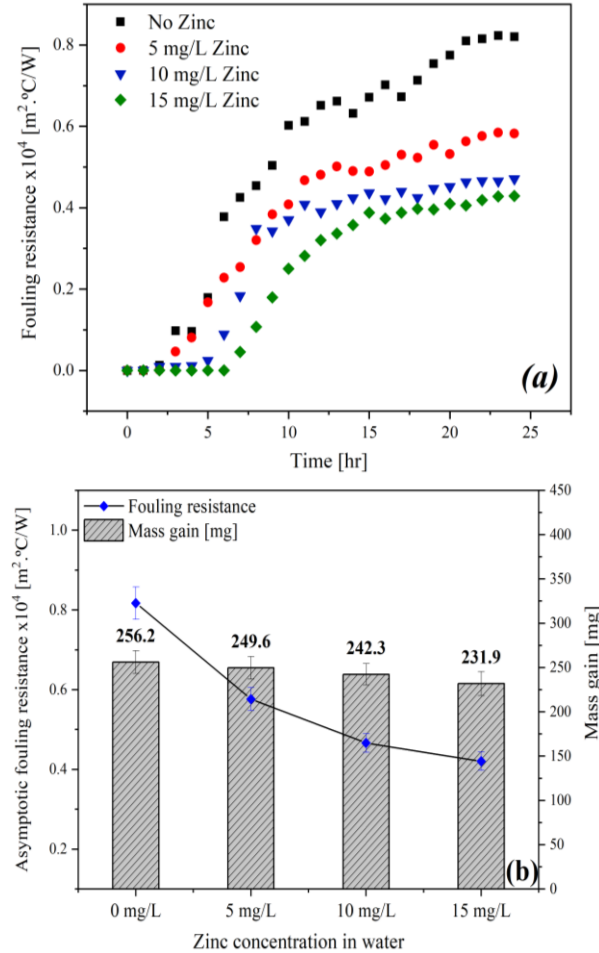


Figure 8 (a) Thermal fouling resistance of scale on the aluminium surface and (b) surface mass gain and asymptotic fouling resistance, for different contents of zinc in water.

Figure 11 shows the elemental analysis (EDX) of the fouling layer for the three tested concentrations. The zinc content of deposits increased from 4.54 wt% to 16.68 wt% as the Zn^{2+} concentration in the solution increased from 5 to 15 mg/L proving the interaction between Zn^{2+} and mineral scale particles. It has been emphasised by Glasner and Weiss [6] that the carbonate complex $[Zn(CO_3)_2]^{2-}$ acts as a nucleation site for $CaCO_3$ crystals. The affinity of Zn^{2+} to the carbonate ions is found greater than Ca^{2+} . Therefore, the combination between Zn^{2+} and CO_3 is more likely at high concentrations of Zn^{2+} forming $[Zn(CO_3)_2]^{2-}$, $Zn_5(CO_3)_2(OH)_6$ or $ZnCO_3$ on the heat transfer surface.

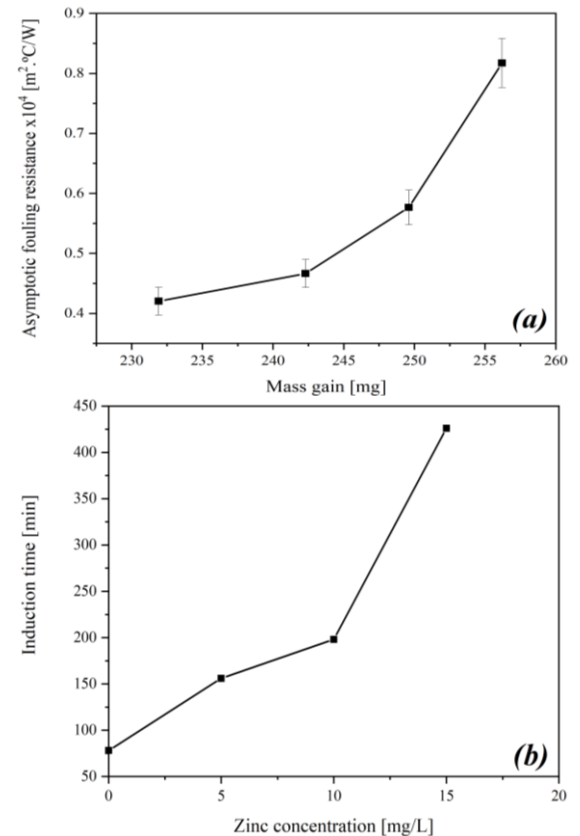
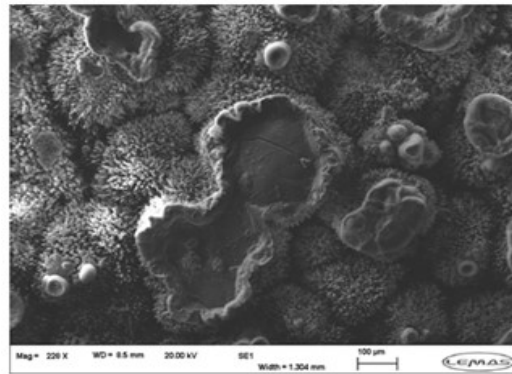


Figure 9. (a) Thermal fouling resistance as a function of scale mass and (b) crystallisation fouling induction time for different concentrations of zinc in water.



(a)



(b)

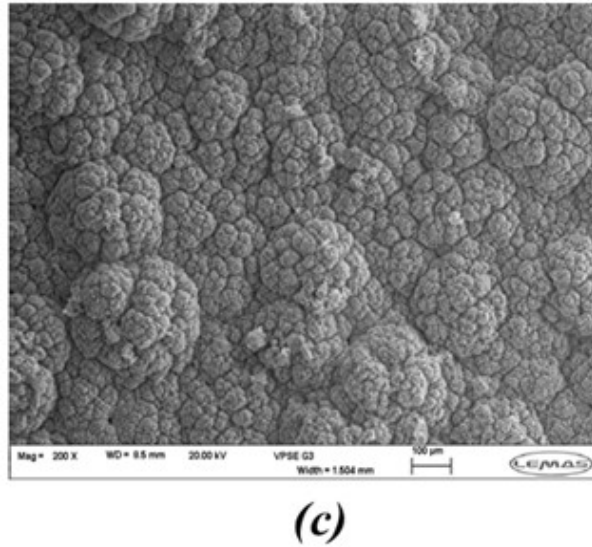


Figure 10. SEM image for deposits on aluminium surface for different concentrations of TOC; (a) no Zinc, (b) $[Zn^{2+}] = 10 \text{ mg/L}$ and (c) $[Zn^{2+}] = 15 \text{ mg/L}$

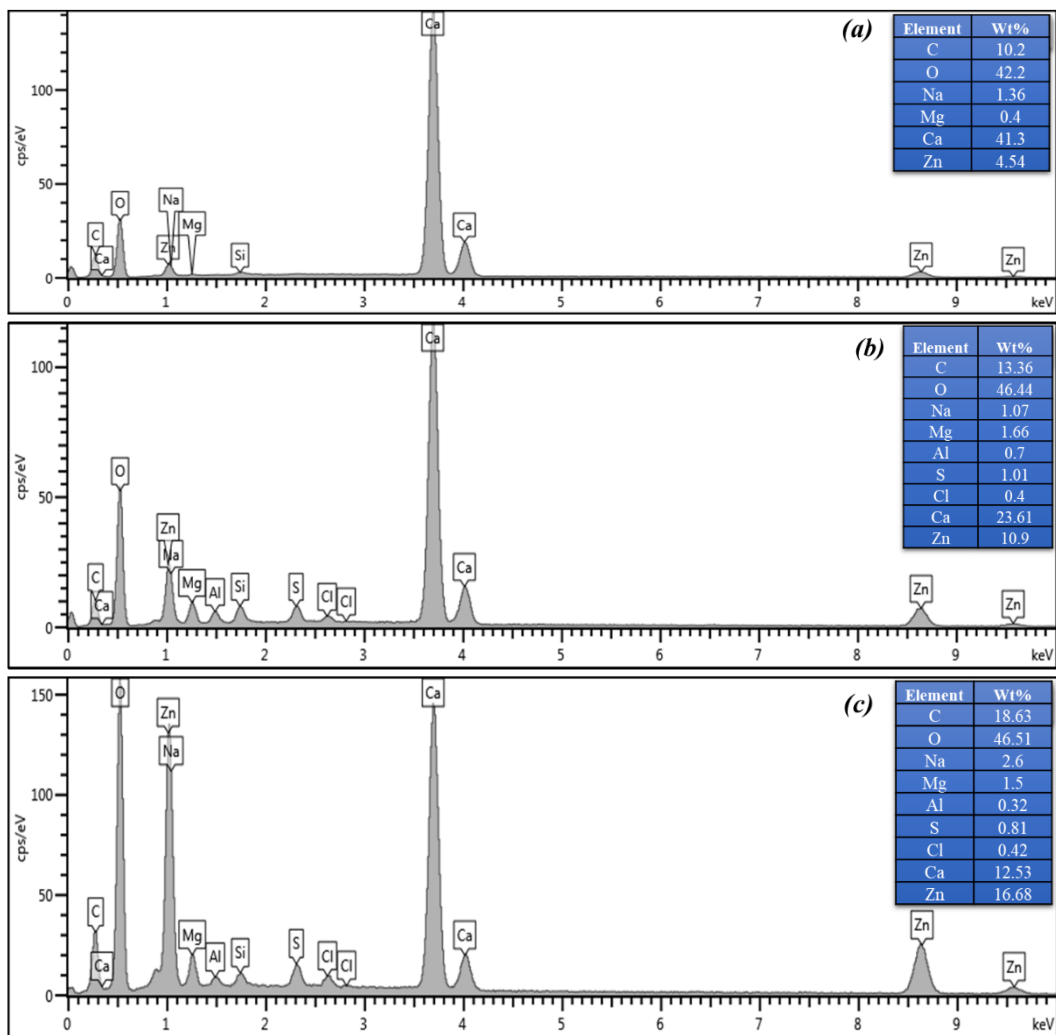


Figure 11. EDX elemental analysis of the deposits on aluminium; (a) $[Zn^{2+}] = 5 \text{ mg/L}$, (b) $[Zn^{2+}] = 10 \text{ mg/L}$ and (c) $[Zn^{2+}] = 15 \text{ mg/L}$.

CONCLUSION

In the present work, the influence of Zn ions in potable water on the kinetics of precipitation and the structure of the scale particles were investigated using a unique batch system associated with the steaming process. Moreover, the fouling rate and morphology of the fouling layer on a heated surface in a once-through flow system were examined. By using a batch steam generator system, the findings showed that the presence of Zn^{2+} reduces the consumption rate of Ca^{2+} during potable water heating. The induction time of $CaCO_3$ crystallisation was prolonged as the content of Zn^{2+} increased. Analysis of Zn^{2+} concentration as a function of time refers to Zn^{2+} consumption either in complexation with other foulants or in the crystallisation reaction to $ZnCO_3$. The presence of $ZnCO_3$ as a smithsonite was confirmed by PXRD analysis. Zn^{2+} in scaling potable water also affects the morphology of the precipitates, changing from fine needles to lumps.

The fouling resistance approach and deposits mass were used to evaluate the influence of zinc on the deposition of the inorganic minerals on the aluminium surface in the open system. The results exhibited that the fouling resistance decreases with the increase of the Zn^{2+} concentration. In terms of fouling morphology, the size of particles reduces significantly due to the impact of Zn^{2+} on the crystal growth. Moreover, the EDX findings showed that the fouling layer content of zinc increases with a solution concentration of Zn^{2+} confirming the deposition of zinc minerals.

ACKNOWLEDGEMENTS

The authors acknowledge the funding and support from the Leeds University SALSAS consortium. We also wish to acknowledge the technical and administrative team of the Institute of Functional Surfaces (IFS), School of Mechanical Engineering at the University of Leeds for their support.

REFERENCES

- [1] H. Meyer, "The influence of impurities on the growth rate of calcite," *J. Cryst. Growth*, vol. 66, no. 3, pp. 639-646, 1984.
- [2] W. H. Organization, "Zinc in Drinking-Water: Background Document for Development of WHO Guidelines for Drinking-Water Quality. 2003," ed, 2003.
- [3] P. Coetzee, Yacoby, M. and S. Howell, "The role of zinc in magnetic and other physical water treatment methods for the prevention of scale," *Water SA*, vol. 22, no. 4, pp. 319-326, 1996.
- [4] J. M. Zachara, J. A. Kittrick, and J. B. Harsh, "The mechanism of Zn^{2+} adsorption on calcite," *Geochimica et Cosmochimica Acta*, vol. 52, no. 9, pp. 2281-2291, 1988/09/01/ 1988, doi: [https://doi.org/10.1016/0016-7037\(88\)90130-5](https://doi.org/10.1016/0016-7037(88)90130-5).
- [5] K. Zeppenfeld, "Prevention of $CaCO_3$ scale formation by trace amounts of copper (II) in comparison to zinc (II)," *Desalination*, vol. 252, no. 1-3, pp. 60-65, Mar. 2010, doi: <https://doi.org/10.1016/j.desal.2009.10.025>.
- [6] A. Glasner and D. Weiss, "The crystallization of calcite from aqueous solutions and the role of zinc and magnesium ions—I. Precipitation of calcite in the presence of Zn^{2+} ions," *J. Inorg. Nucl. Chem.*, vol. 42, no. 5, pp. 655-663, 1980.
- [7] A. Al-Gailani, O. Sanni, T. V. J. Charpentier, R. Crisp, J. H. Bruins, and A. Neville, "Examining the effect of ionic constituents on crystallization fouling on heat transfer surfaces," *International Journal of Heat and Mass Transfer*, vol. 160, p. 120180, 2020/10/01/ 2020, doi: <https://doi.org/10.1016/j.ijheatmasstransfer.2020.120180>.
- [8] A. Al-Gailani, T. V. Charpentier, O. Sanni, and A. Neville, "Crystallization fouling in domestic appliances and systems," *Heat Transfer Engineering*, pp. 1-10, 2021.
- [9] S. Ghizellaoui, M. Euvrard, J. Ledion, and A. Chibani, "Inhibition of scaling in the presence of copper and zinc by various chemical processes," *Desalination*, vol. 206, no. 1-3, pp. 185-197, 2007.
- [10] B. Pernot, M. Euvrard, F. Remy, and P. Simon, "Influence of Zn (II) on the crystallisation of calcium carbonate application to scaling mechanisms," *Aquatic Journal of Water Services Research and Technology*, vol. 48, no. 1, pp. 16-23, 1999.
- [11] S. Ghizellaoui and M. Euvrard, "Assessing the effect of zinc on the crystallization of calcium carbonate," *Desalination*, vol. 220, no. 1-3, pp. 394-402, 2008.
- [12] W. Stumm and J. J. Morgan, *Aquatic chemistry: chemical equilibria and rates in natural waters*. John Wiley & Sons, 2012.
- [13] L. Wenjun, F. Hui, J. Lédion, and W. Xingwu, "Anti-scaling properties of zinc ion and copper ion in the recycling water," *Ionics*, vol. 15, no. 3, pp. 337-343, 2009.
- [14] knovel, "Physical Constants of Inorganic Compounds," ed, 2020.
- [15] E. Abouali, O. Jean, and J. Lédion, "Influence du cuivre et du zinc sur le

- pouvoir entartrant de l'eau," *Journal européen d'hydrologie*, vol. 27, no. 2, pp. 109-126, 1996.
- [16] H. J. Meyer, "The influence of impurities on the growth rate of calcite," *J. Cryst. Growth*, vol. 66, no. 3, pp. 639-646, 1984/05/01/ 1984, doi: [https://doi.org/10.1016/0022-0248\(84\)90164-7](https://doi.org/10.1016/0022-0248(84)90164-7).
- [17] R. Sabzi and R. Arefinia, "Investigation of zinc as a scale and corrosion inhibitor of carbon steel in artificial seawater," *Corros. Sci.*, vol. 153, pp. 292-300, 2019/06/01/ 2019, doi: <https://doi.org/10.1016/j.corsci.2019.03.045>.